

Article

Assessment of Thermal Performance of Phase-Change Material-Based Multilayer Protective Clothing Exposed to Contact and Radiant Heat

Morgan Renard, Waldemar Machnowski  and Adam K. Puszkarz * 

Lodz University of Technology, Faculty of Material Technologies and Textile Design, Institute of Material Science of Textiles and Polymer Composites, 116 Żeromskiego Street, 90-924 Lodz, Poland; 230255@edu.p.lodz.pl (M.R.); waldemar.machnowski@p.lodz.pl (W.M.)

* Correspondence: adam.puszkarz@p.lodz.pl

Abstract: The research presented in this article concerns the thermal properties of multilayer protective clothing, specifically, the impact of phase-change material (PCM) incorporation on the occurring heat transfer. Multilayer textile assemblies with PCM inserts (macrocapsules containing n-octadecane) and reference assemblies with PP inserts (macrogranules from polypropylene) with very similar geometry and the same textile layers were tested. The spatial geometry of tested assemblies was examined using high-resolution X-ray microtomography (micro-CT). The heating process of the assemblies was examined under the conditions of exposure to contact heat (using thermography) and radiant heat (using a copper plate calorimeter, according to EN ISO 6942). PCM-containing assemblies achieved a temperature rise of 12 °C in a longer period than the reference assemblies; for the contact heat method, the time was longer by 11 and 14 min, and for the radiant heat method by 1.7 and 2.1 min.

Keywords: phase-change materials; PCMs; heat transfer; contact heat; radiant heat; thermography; micro-CT



Citation: Renard, M.; Machnowski, W.; Puszkarz, A.K. Assessment of Thermal Performance of Phase-Change Material-Based Multilayer Protective Clothing Exposed to Contact and Radiant Heat. *Appl. Sci.* **2023**, *13*, 9447. <https://doi.org/10.3390/app13169447>

Academic Editor: Alberto Corigliano

Received: 5 July 2023

Revised: 2 August 2023

Accepted: 16 August 2023

Published: 21 August 2023



Copyright: © 2023 by the authors. Licensee MDPI, Basel, Switzerland. This article is an open access article distributed under the terms and conditions of the Creative Commons Attribution (CC BY) license (<https://creativecommons.org/licenses/by/4.0/>).

1. Introduction

One of the many ways of storing heat is by phase change. A phase transition is an isothermal thermodynamic process caused by a change in ambient temperature or pressure. As a result of the change in state aggregation (e.g., melting–solidification), phase-change materials (PCMs) can absorb, store, and release energy in the form of latent heat at a constant temperature, called the phase transition temperature. The amount of heat absorbed (and stored) during the heating of a typical material (non-PCM) is much less than the amount of heat absorbed (and accumulated) during the phase transformation (melting) of this material. When analyzing the possibility of using a given type of PCM as a material that absorbs and accumulates heat, four key essential properties should be taken into account: (1) *Heat capacity*, i.e., the ability to accumulate heat of PCM materials, depending primarily on the heat of phase transition; (2) *Phase transition temperature*, i.e., the temperature at which the PCM absorbs the largest amount of energy (and accumulates and releases it to the environment). The type of phase-change material should be selected so that its phase-change temperature is within the temperature range of the environment in which it will be used; (3) *Thermal conductivity*, i.e., the ability of PCMs to effectively absorb and release heat, even in conditions of small temperature differences between the system and the environment. This condition is met by PCMs with high thermal conductivity; (4) *Thermal property stability*. For the PCM to work effectively multiple times, it should retain its thermal properties over many melt–solid cycles [1–3].

For decades, PCMs, due to their useful properties, have been widely used as heat accumulators in installations using renewable energy sources (in particular solar

radiation energy-photovoltaic modules) [4–7]; heat insulators in structural elements of buildings [8–13]; temperature stabilizers of food products or medicines (isothermal containers) [14–16]; temperature stabilizers of road surfaces [17–19]. The use of these materials in multilayer wall structures results in a reduction in daily temperature amplitudes inside the building and a delay in releasing the stored heat. In the case of building applications, the PCMs used possess a phase-change temperature within the temperature range outside the building (extreme temperatures in a daily cycle) and the temperature range of thermal comfort inside the building. PCMs are also commonly and successfully used in heat-insulating clothing, designed especially for work in extreme thermal conditions. Both in very low and very high ambient temperatures, an important problem is to simultaneously ensure effective protection against the harmful effects of the cold/heat and ensure the ergonomics of clothing [20–30]. This clothing is usually made of thick, multi-layered textile systems, which significantly reduces the user's freedom of movement and prevents him from effective and precise work [31]; in addition, during intense physical exertion, these garments often become wet due to the secretion of sweat by the wearer, which in turn reduces their thermal insulation and increases the feeling of discomfort [32–37]. Figure 1 shows a schematic comparison of the PCM vs. non-PCM heating process.

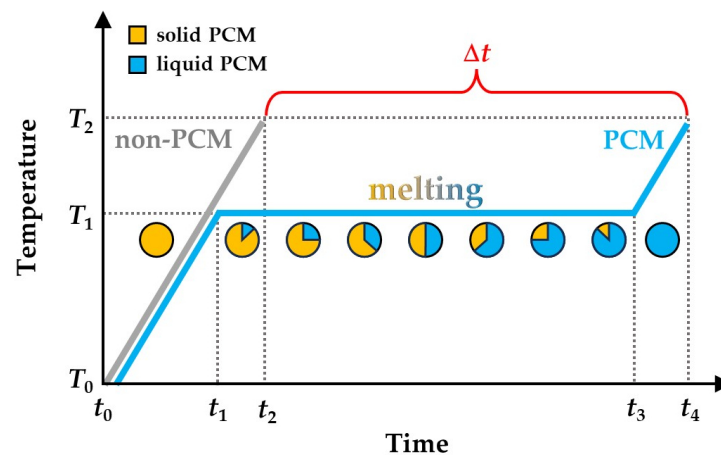


Figure 1. Comparison of PCM and non-PCM heating processes.

The process starts at time t_0 , when the initial temperature of both materials is T_0 . At time t_1 , both materials reach the temperature T_1 , which for the PCM is the phase transition temperature. At time t_1 , melting of the PCM starts and continues until time t_3 is reached. During this time, the temperature of the PCM does not rise because all the heat supplied to the material is converted into a change in state of the PCM. At time t_3 , the PCM is completely melted, and its temperature starts to rise again to reach the value of T_2 at time t_4 . In the case of non-PCM, the heating process is faster and reaches the temperature T_2 at time t_2 . The scheme shows the time gain, $\Delta t = t_4 - t_2$, i.e., the difference in the heating time of both materials needed to reach T_2 . From a practical point of view, temperature T_2 may be a critical value that should not be exceeded. For example, T_2 can be the maximum temperature:

- Of the internal wall of a building, for which the temperature inside is within the range ensuring the thermal comfort of the residents;
- At which food or drugs can be stored, and the use of PCMs in their packaging can extend the transport time without the risk of deterioration of their properties;
- Of the inner layer of clothing containing PCMs for which the skin of the wearer will not burn.

The Δt may take different values because it depends on the type and amount of PCM used in the tested system.

The aim of the research described in this current article was to investigate the potential use of inserts containing PCM macrocapsules in multilayer protective clothing. The results of the PCM efficiency evaluation were compared with analogous multilayer clothing assemblies with similar geometry with PP macrogranules (non-PCM). The research involved the analysis of heat transfer through textile assemblies under conditions of exposure to contact heat and radiant heat.

2. Materials and Methods

2.1. Materials

The subjects of the research were PCM macrocapsules (Microtek Laboratories, Moraine, OH, USA). The macrocapsules were spherical in shape, with a diameter: 4 ± 0.5 mm. According to the manufacturer's information, the outer shell of the macrocapsules was polyurethane (PU), while the PCM material was n-octadecane. Based on high-resolution X-ray tomography, micro-CT (SkyScan 1272; Bruker, Kontich, Belgium), and scanning electron microscopy, Nova NanoSEM 230 (FEI, Eindhoven, The Netherlands), the internal structure of macrocapsules was characterized. Both applied techniques showed that PCM macrocapsules are formed from multiple PCM microcapsules (with maximum diameter of about $50 \mu\text{m}$); moreover, PU, which constitutes 21% of volume of the macrocapsule, forms both the outer shell of the macrocapsules (with maximum thickness of $155 \mu\text{m}$) and the outer shell of the microcapsules. The remaining 79% of volume of the macrocapsule is n-octadecane. Figure 2a presents a micro-CT image of macrocapsule's cross section and the SEM cross-section image of macrocapsule's interior with visible microcapsules. As a reference material for the tested PCM macrocapsules, macrogranules of similar geometry made of PP were used (the obtained cross-section image using micro-CT was presented in Figure 2b).

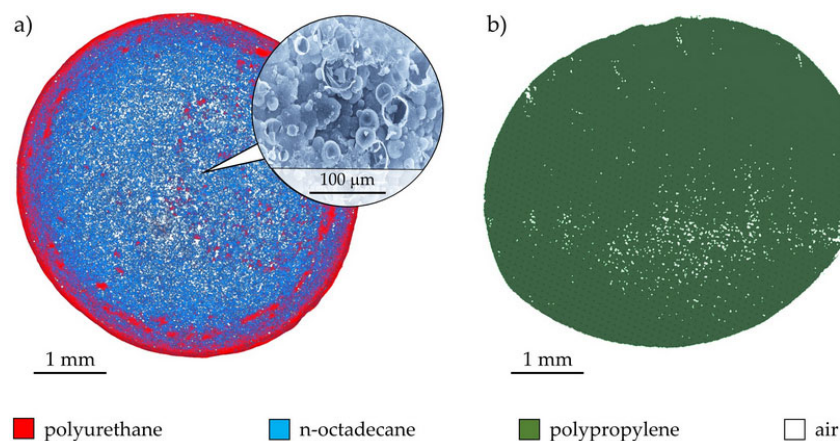


Figure 2. Cross section of PCM macrocapsule (a), and PP macrogranule (b).

Both PCM macrocapsules and PP macrogranules are characterized by low porosity. In the case of macrocapsules, air (white color) constitutes 4% of their volume, filling micropores of a maximum size of $175 \mu\text{m}$. In the case of macrogranules, air constitutes 3% of their volume and fills the micropores of a maximum size of $65 \mu\text{m}$. As can be seen in the presented cross sections, the spatial distribution of pores is more homogeneous in the case of PCM macrocapsules. N-octadecane used as PCM in the tested macrocapsules is characterized by a melting temperature of $28 \text{ }^\circ\text{C}$, heat of fusion of $185 \text{ J}\cdot\text{g}^{-1}$, with specific heats of $1.9 \text{ kJ}\cdot\text{kg}^{-1}\cdot\text{K}^{-1}$ (solid phase), and $2.2 \text{ kJ}\cdot\text{kg}^{-1}\cdot\text{K}^{-1}$ (liquid phase). Since the aim of the work was to test the thermal insulation properties of PCM macrocapsules for potential use in thermal protective clothing, an insert containing a monolayer of these macrocapsules (arranged next to each other wrapped in white polyester mesh) was created. Additionally, reference insert containing PP macrogranules was made. Photos of both inserts are shown in Figure 3, while their structural and thermal parameters are presented in Table 1.

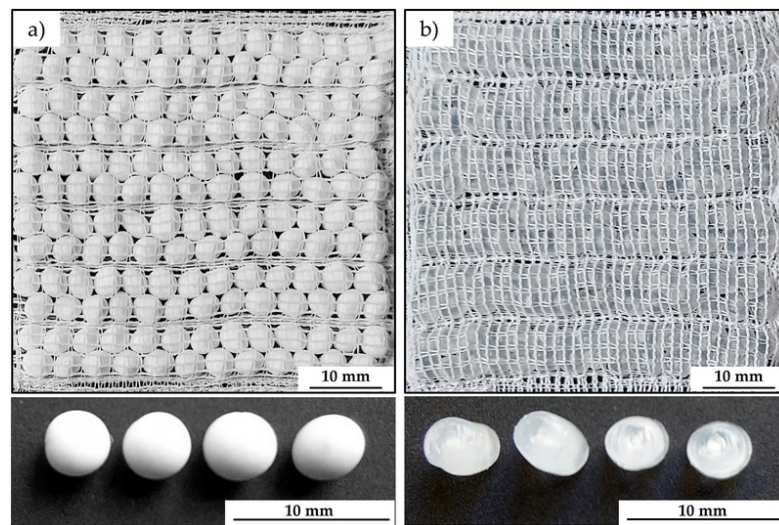


Figure 3. Photos of inserts containing: (a) PCM macrocapsules, (b) PP macrogranules (reference).

Table 1. Structural and thermal properties of tested inserts.

Insert	Insert Composition	Raw Material	Specific Heat [kJ·kg ⁻¹ ·K ⁻¹]	Melting Temperature [°C]	Heat of Fusion [kJ·kg ⁻¹]	Thickness [mm]	Porosity [%]
PCM	macrocapsules	n-octadecane (79%) polyurethane (21%)	1.9 (solid)/2.2 (liquid) 1.1	28 250	185	4.47	4
	PES mesh	polyester (100%)	1.4	260	not applicable	0.31	87
PP	macrogranules	polypropylene (100%)	1.7	165	not applicable	4.13	3
	PES mesh	polyester (100%)	1.4	260	not applicable	0.31	87

As can be seen in Figure 3, both inserts were approximately 5 cm × 5 cm large and consisted of about 160 macrocapsules/macrogranules. The PCM macrocapsules were opaque white, while the PP macrogranules were colorless.

Thermal barriers in protective clothing are most commonly made of nonwoven fabrics. In their place, a PCM insert was used, in two multilayer textile assemblies (A and C), due to its high usefulness in thermal insulation systems. As references for assemblies A and C, assemblies B and D were created, respectively, identical in terms of the structure of all layers, except for their thermal barriers, where instead of PCM macrocapsules inserts, inserts with PP macrogranules were used. All four assemblies, the full characteristics of which are presented in Table 2, consisted of four basic layers: (1) outer shell, (2) moisture barrier, (3) thermal barrier, and (4) lining. The outer shell is most resistant to mechanical impact and protects the wearer against hot and toxic substances. The moisture barrier provides protection against the permeation of water and other liquids, including volatile chemicals that could penetrate the outer shell. The moisture barrier also provides a key role in the breathability and insulation of the entire multilayer assembly. It usually consists of two parts, a vapor-permeable membrane and a substrate (e.g., nonwoven fabric, woven fabric), with which the membrane is bonded. The thermal barrier, due to its high porosity and greatest thickness, provides the best thermal insulation of all layers. The smooth lining ensures easy and quick dressing and undressing.

Table 2. Characteristics of four tested assemblies.

Assembly	Layer Type	Textile	Weave	Raw Material	Thickness [mm]	Surface Mass [$\text{g}\cdot\text{m}^{-2}$]	Porosity [%]	Yarn Porosity [%]	
A	Outer shell	Woven fabric 1	plain	aramid	0.495	199	67	31	
	Moisture barrier	Membrane 1	-	polyurethane	0.066	155	0.05	-	
		Nonwoven fabric 1	-	aramid	0.830		90	-	
	Thermal barrier	PCM insert	-	polyurethane n-octadecane polyester	4.467	6.269	1548	67	75
Lining	Woven fabric 2	plain	aramid	0.411		192	47	12	
B	Outer shell	Woven fabric 1	plain	aramid	0.495	199	67	31	
	Moisture barrier	Membrane 1	-	polyurethane	0.066	155	0.05	-	
		Nonwoven fabric 1	-	aramid	0.830		90	-	
	Thermal barrier	PP insert	-	polypropylene polyester	4.438	6.240	1308	70	78
Lining	Woven fabric 2	plain	aramid	0.411		192	47	12	
C	Outer shell	Woven fabric 1	plain	aramid	0.495	199	67	31	
	Moisture barrier	Membrane 2	-	polyurethane	0.032	115	0.07	-	
		Nonwoven fabric 2	-	aramid	0.486		79	-	
	Thermal barrier	PCM insert	none	polyurethane n-octadecane polyester	4.467	5.891	1548	67	70
Lining	Woven fabric 2	plain	aramid	0.411		192	47	12	
D	Outer shell	Woven fabric 1	plain	aramid	0.495	199	67	31	
	Moisture barrier	Membrane 2	-	polyurethane	0.032	115	0.07	-	
		Nonwoven fabric 2	-	aramid	0.486		79	-	
	Thermal barrier	PP insert	-	polypropylene polyester	4.438	5.862	1308	70	74
Lining	Woven fabric 2	plain	aramid	0.411		192	47	12	

Figure 4 shows the optical microscopy (Delta Optical Smart 5MP PRO made by Delta Optical, Warsaw, Poland) images of both sides of the textiles forming the 4 tested assemblies, while Figure 5 additionally shows 3D micro-CT images of the same textiles as well as 3D micro-CT images of the 4 tested assemblies: A, B, C, and D.

On this basis, the plain weave of both fabrics forming the outer shell (woven fabric 1) and the lining (woven fabric 2) can be clearly identified (Figures 4a–d and 5a–d). In addition, both figures clearly show two-sided openings in the nonwoven fabric 1, forming a moisture barrier in assemblies A and B (Figures 4e and 5e). These openings increased nonwoven fabric 1 porosity (90%), which resulted in thermal insulation increase.

Based on the 3D micro-CT images of the 4 tested assemblies (reduced to a surface size of $1\text{ cm} \times 1\text{ cm}$ to improve the identification of all layers), shown in Figure 5 and the data in Table 2, it can be seen that the assemblies containing PCM inserts (A and C) and the reference assemblies with PP inserts (B, D) differ only in the moisture barrier. In assemblies A and B, the moisture barrier was formed of a membrane 1 and a nonwoven fabric 1, while in assemblies C and D, the moisture barrier was formed of a membrane 2 and a nonwoven fabric 2. The above selection of textiles forming the moisture barrier in the

tested assemblies was intended to clearly distinguish the pair of assemblies *A* and *C* from the pair of assemblies *B* and *D* in terms of spatial structure. Nonwoven fabric 2 forming the moisture barrier in assemblies *C* and *D* was 52% thinner and 12% less porous than the nonwoven fabric 1, forming the moisture barrier in assemblies *A* and *B*.

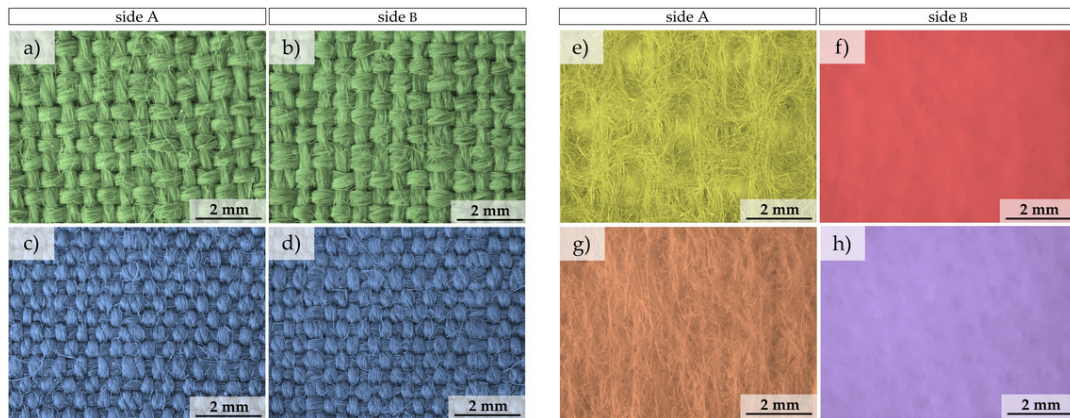


Figure 4. Optical microscopy images of both sides of the textiles forming the 4 tested assemblies: (a,b) woven fabric 1; (c,d) woven fabric 2; (e) nonwoven fabric 1; (f) membrane 1; (g) nonwoven fabric 2; (h) membrane 2.

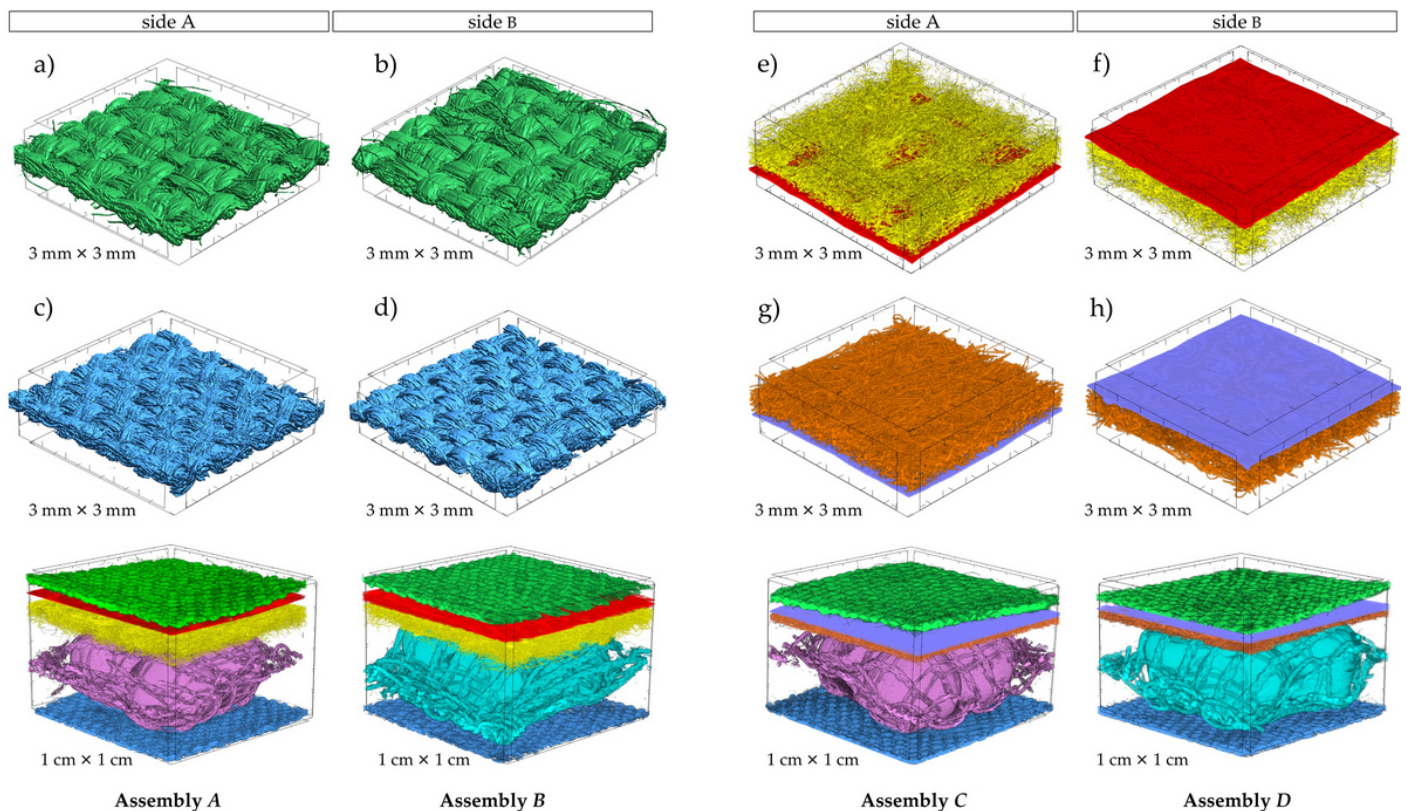


Figure 5. The 3D micro-CT images of both sides of the textiles forming the 4 tested assemblies: (a,b) woven fabric 1; (c,d) woven fabric 2; (e) nonwoven fabric 1; (f) membrane 1; (g) nonwoven fabric 2; (h) membrane 2. In the bottom row, 3D micro-CT images of all 4 tested assemblies: *A*, *B*, *C*, *D*.

2.2. Methods

To assess the potential application of PCM macrocapsules in multilayer thermal insulation protective clothing, assemblies *A* and *C* were subjected to two independent experi-

ments, in which heat transfer was induced through the tested assemblies (by contact heat and radiant heat). The test results were compared with the experiment results performed for reference assemblies (B and C) containing PP macrogranules. Schemes of the measurement systems for both applied experimental methods are shown in Figure 6. The physical phenomena that are the basis of these methods correspond to the actual thermal hazards to which the wearer is exposed (contact with hot bodies or exposure to intense thermal radiation), which makes it possible to properly assess the basic properties of thermal protective clothing.

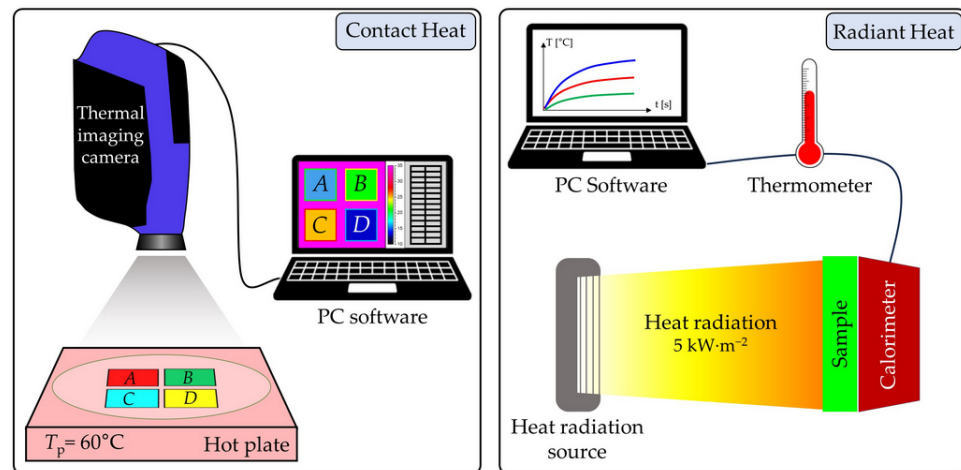


Figure 6. Schemes of the measurement system for both applied experiments.

2.2.1. Contact Heat

The experiment was carried out with a constant ambient temperature $T_a = 24\text{ }^\circ\text{C}$. In this method, the tested assemblies were placed (with the outer shell facing down) on a flat horizontal surface of a hot plate (e-G51HP07C Guardian 5000 model, OHAUS Europe GmbH, Nänikon, Switzerland) with a constant temperature: $T_p = 60\text{ }^\circ\text{C}$. As a result of direct contact of the outer layer of the assembly with the hot plate's surface, all layers of the assemblies gradually heated up, starting from the outer layer (being in direct contact with the hot plate), then through the moisture barrier, thermal barrier, to the lining (farthest from the hot plate). The process of heating the upper surface of the lining was measured over time using a thermal imaging camera (FLIR SC 5000 model made in Wilsonville, OR, USA) placed above the hot plate and recorded in form of thermograms by Altair—Thermal Image Analysis Software, version 5.90.001. To unify the measuring method of lining temperature (with a thermal imaging camera), the lining of each tested assembly was always the same textile material (i.e., woven fabric 2; see Table 2) with the same emissivity (resulting from the identical microstructure and raw material composition). The temperature range (24–60 °C) in which the experiment was run included the melting point of the phase-change material used (28 °C); in addition, the selected temperature range allowed us to observe the similarity of the heating process of the tested assemblies containing the PCM insert to the scheme shown in Figure 1 and allowed to clearly observe three stages of heating of the PCM macrocapsules (as solid, as solid and liquid, as liquid). Moreover, according to medical knowledge, heating the human skin to a temperature above 55 °C causes discomfort or pain, and after a few minutes skin damage; therefore, the standards regarding thermal hazards in any environment, e.g., in the workplace, in the home (EN 563 [38], EN ISO 13732-1 [39]) provide temperature threshold values for burns that occur when human skin is in contact with a hot solid surface. The threshold value for burns for metal smooth surfaces it is determined at the level of approx. 60 °C.

The experiment was carried out until a steady state was reached by all assemblies when the temperature of the lining T_L reached the maximum possible and constant value over time.

2.2.2. Radiant Heat

The experiments were carried out according to EN ISO 6942 [40] under the same ambient conditions as the contact heat experiment. In this method, the tested assemblies—oriented in a vertical position—were exposed to thermal radiation, which was emitted by a source generating a heat flux of $5 \text{ kW}\cdot\text{m}^{-2}$ and fell on the outer shell of the assembly causing it to heat up. The $5 \text{ kW}\cdot\text{m}^{-2}$ relatively low radiation intensity is at the level of incident heat flux density to which industrial workers and fire fighters may be exposed. As a result, the process of heating subsequent layers took place through the moisture barrier, through the thermal barrier, to the lining. The process of heating the lining was measured over time using a copper sensor of the calorimeter connected to a digital, computer-driven thermometer. To unify the measuring method of lining temperature (with a calorimeter), for each tested assembly the lining was always the same textile material (i.e., woven fabric 2; see Table 2) with the same surface microstructure, ensuring identical contact with the copper plate. Results of measurements of the average temperature of the lining were recorded in 1 s intervals until its temperature increased to $50 \text{ }^\circ\text{C}$.

3. Results and Discussion

3.1. Contact Heat

In Figure 7, the temperatures displaying the tested linings' dependence on the exposure time of the outer shell to the contact heat are presented.

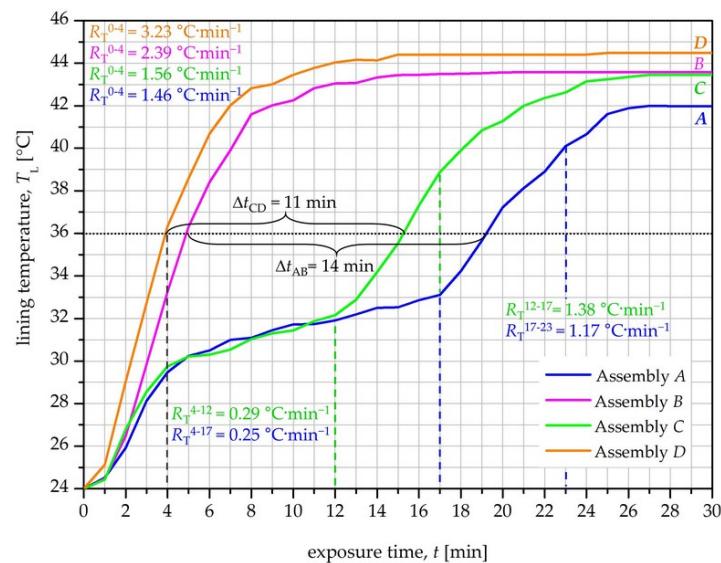


Figure 7. Lining temperature versus exposure time of the outer shell to contact heat.

This chart shows a clear difference in the heating process of assemblies based on phase-change materials (A and C) and assemblies based on reference materials (B and D). The first difference between the above-mentioned kinds of samples is already visible in the initial stage of the heating process (in the first 4 min). In this stage, the temperature of all tested assemblies increases linearly over time. Assemblies containing PCMs heat up more slowly than their counterparts containing PP macrogranules. The temperature rise rate R_T^{0-4} during this stage is $1.46 \text{ }^\circ\text{C}\cdot\text{min}^{-1}$ (assembly A) and $1.56 \text{ }^\circ\text{C}\cdot\text{min}^{-1}$ (assembly C), while for assemblies B and D are $2.39 \text{ }^\circ\text{C}\cdot\text{min}^{-1}$ and $3.23 \text{ }^\circ\text{C}\cdot\text{min}^{-1}$, respectively. It should be assumed that the observed lower R_T^{0-4} values for PCM-containing assemblies are due to the fact that already after about 1 min of exposure time, some amount of the n-octadecane content in PCM macrocapsules warms up to melting temperature ($28 \text{ }^\circ\text{C}$). As a consequence, a slow isothermal melting process of n-octadecane begins. It should be noted that the lower parts of the PCM macrocapsules (closest to the hot plate) are heated to melting temperature ($28 \text{ }^\circ\text{C}$) earlier than the lining is. As can be seen in Figure 7, the lining of the PCM-containing

assemblies reaches 28 °C in the third minute of exposure time. After the fourth minute of exposure time, a clear difference in the temperature increase between PCM-containing assemblies and PP-containing assemblies was observed. In contrast to assemblies *A* and *C*, for which a second slower heating stage can be distinguished, assemblies *B* and *D* heat up at a rate comparable to that of the first stage. This means that, in PCM-containing assemblies, when the entire amount of n-octadecane reaches the melting temperature, intensive melting of the octadecane occurs as a result, which absorbs a significant part of the heat flux generated by the hot plate. In this stage of the heating process, the temperature rise rate of the lining is milder than in the previous heating stage, $R_T^{4-17} = 0.25 \text{ }^\circ\text{C}\cdot\text{min}^{-1}$ for assembly *A* and $R_T^{4-12} = 0.29 \text{ }^\circ\text{C}\cdot\text{min}^{-1}$ for assembly *C*. For assembly *A*, this stage lasts from 4 min to 17 min, while for assembly *C* from 4 min to 12 min. The five-minute difference is due to the different construction of the nonwoven fabric in these assemblies. Assembly *A*, in which there is a thicker and more porous nonwoven fabric (1) than in assembly *C* (nonwoven fabric 2), due to its greater thermal insulation, created a more effective barrier to the heat flux passing from the thermal barrier to the lining. The third stage of the heating process (starting for assembly *A* at the seventeenth minute while for assembly *C* at the twelfth minute), is characterized by a higher temperature rise rate of the lining compared to the second stage. At this stage, the entire amount of n-octadecane has melted, and the heat generated by the hot plate is not absorbed for the n-octadecane phase transition but is entirely converted into a temperature increase in the assemblies. To compare the effectiveness of thermal insulation of the assemblies containing PCMs inserts (*A* and *C*) with the reference assemblies containing PP inserts (*B* and *D*), the time gains Δt_{AB} and Δt_{CD} —the time difference in which the respective assemblies reached the temperature of 36 °C—were calculated (indicated in Figure 7). An important parameter of thermal protective clothing quality is the parameter expressing the clothing exposure time in which the temperature of the inner layer of clothing increases by 12 °C (EN ISO 6942); therefore, on the basis of the course of the curves in Figure 8, the values of Δt_{AB} and Δt_{CD} (14 and 11 min, respectively) were calculated for the increase in lining temperature based on the curves from Figure 8. As can be seen in the chart presented in Figure 7 and on the thermograms (Figure 8), in the ninth minute of the exposure time of assemblies *A* (with PCMs insert) and *B* (with PP insert), the highest difference in the lining temperature ΔT_L^{AB} was obtained (10.5 °C).

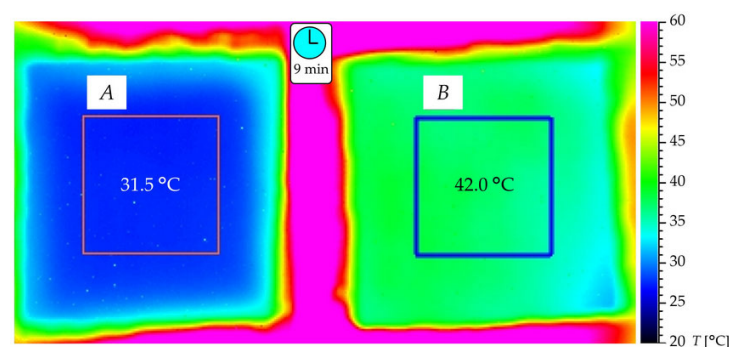


Figure 8. Thermograms of assemblies *A* and *B* obtained in ninth minute of the heating process.

Both thermographs show the central fragment of the lining surface (a square with a side length of about 3 cm), inside which the thermal imaging camera measured the average temperature of the lining during the process of heating of tested assemblies. The square area was chosen in such a way as to avoid the adverse influence of the boundary conditions (visible on the side edges of the lining resulting from the cooling of the samples by the ambient air) on the temperature measurement.

3.2. Radiant Heat

In Figure 9, the temperatures of tested linings' dependence, t , on the exposure time of the outer shell to radiant heat are presented.

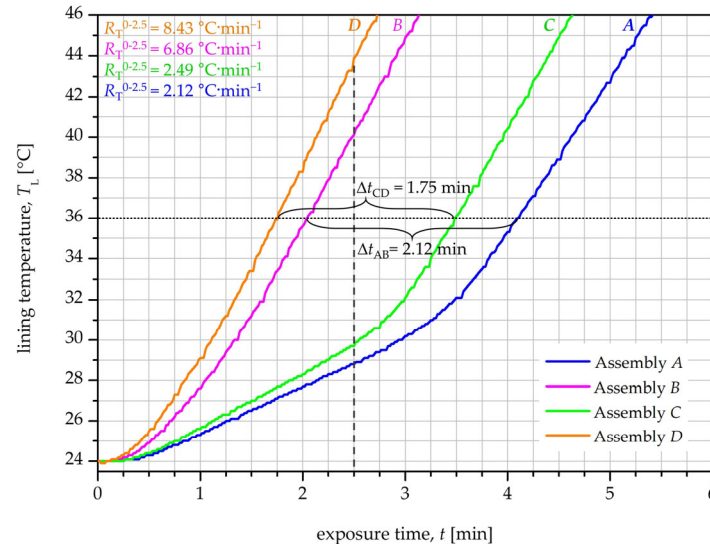


Figure 9. Lining temperature versus exposure time of the outer shell to radiant heat.

The chart shows a pronounced difference in the heating process of assemblies containing phase-change materials (A and C) and reference assemblies (B and D). As one can easily see, the assemblies with inserts containing PP macrogranules heat up much faster. The course of the curves showing the temperature increase in assemblies containing PCM inserts can be divided into two stages. The first stage lasts for about 2.5 min of the experiment. At this stage, a significantly lower temperature rise rate $R_T^{0-2.5}$ of these assemblies can be observed ($2.12 \text{ }^\circ\text{C}\cdot\text{min}^{-1}$ for assembly A, $2.49 \text{ }^\circ\text{C}\cdot\text{min}^{-1}$ for assembly C) compared to the corresponding reference samples ($6.86 \text{ }^\circ\text{C}\cdot\text{min}^{-1}$ for assembly B, $8.43 \text{ }^\circ\text{C}\cdot\text{min}^{-1}$ for assembly D). The reason for the slower heating of the PCM-containing assemblies was the isothermal phase transition (melting) of n-octadecane, which was ongoing at this stage of the experiment. Due to the significantly higher heat flux in the radiant heat method compared to the *contact heat* method, in Figure 9, the two-stage process of the temperature increase during the phase transition of n-octadecane was not revealed (which was revealed in Figure 8). As one can see in Figure 9, the applied radiant heat flux ($5 \text{ kW}\cdot\text{m}^{-2}$) used in this method caused—after about 15 s (0.25 min), in both assemblies (A, C)—the entire amount of n-octadecane to reach the melting temperature. As a result, intensive melting of the n-octadecane occurred. The time interval (0–0.25 min) is the time taken for the heat to transfer from the outer shell (exposed to radiant heat) to the lining. Similarly, for the contact heat method on the basis of the course of the curves, the values of time gains, Δt_{AB} and Δt_{CD} (2.12 and 1.75 min, respectively), were calculated and are marked in Figure 9.

4. Conclusions

This article presents an attempt to use inserts containing macrocapsules with a phase-change material—n-octadecane with a melting point of $28 \text{ }^\circ\text{C}$ —in multilayer textile assemblies used in thermal protective clothing. The results obtained for both applied methods to assess the effectiveness of using PCM-macrocapsules as a thermal barrier allow us to formulate the following conclusions:

- Both applied test methods (*contact heat* and *radiant heat*) showed that the use of PCM-containing inserts clearly slows down the heating process of multilayer textile assemblies in comparison to the reference assemblies containing PP macrogranules;

- According to the results of the *contact heat* method, the use of PCM inserts in a certain period of exposure to heat, leads to a ten-fold slowdown in the rate of assemblies heating compared to reference assemblies. As a result, the PCM-containing assemblies reached a temperature increase of 12 °C in a longer time (11 min or 14 min) compared to the PP macro-granular assemblies. As can be seen on the chart (Figure 8), the temperature increase time of the PCM-containing assemblies by 12 °C is about 270% longer compared to the reference assemblies;
- Results of the *radiant heat* method show that the use of PCM inserts in a certain period of exposure to heat leads to a ten-fold slowdown in the rate of assemblies heating compared to reference assemblies. As a result, the PCM-containing assemblies reached a temperature increase of 12 °C in a longer time (1.75 min or 2.12 min) compared to the PP macro-granular assemblies. As can be seen on the chart (Figure 9), the temperature increase time of the PCM-containing assemblies by 12 °C is about 100% longer compared to the reference assemblies;
- Based on the obtained temperature increase characteristics of tested assemblies, one can observe the high efficiency of PCM macrocapsules as a means of improving thermal insulation. The tested PCM macrocapsules could be successfully used in thermal protective clothing and provide the wearer with thermal comfort and effective protection against skin burns.

Author Contributions: M.R.: Methodology, data curation, validation, formal analysis, writing—original draft preparation; W.M.: Methodology, data curation, formal analysis, writing—original draft preparation; A.K.P.: Conceptualization, data curation, visualization, formal analysis, writing—original draft preparation. All authors have read and agreed to the published version of the manuscript.

Funding: This study was financed by funds assigned from: I42/501-4-42-1-1 statutory activity by the Lodz University of Technology, Institute of Material Science of Textiles and Polymer Composites, Poland; the “Innovative Textiles 2020+” No. RPLD. 01.01.00-10-0002/17-00 investment project within the Regional Operational Programme for Łódzkie 2014–2020.

Institutional Review Board Statement: Not applicable.

Informed Consent Statement: Not applicable.

Data Availability Statement: Not applicable.

Acknowledgments: This article is based on the results of the MSc thesis entitled “Evaluation of thermal properties of multilayer protective clothing containing phase change materials” by Morgan Renard.

Conflicts of Interest: The authors declare no conflict of interest.

References

1. Phase Change Materials (PCM) in Construction—Properties and Types. Available online: <https://www.izolacje.com.pl/artykul/chemia-budowlana/157086,materialy-zmiennofazowe-pcm-w-budownictwie-wlasciwosci-i-rodzaje> (accessed on 2 July 2023).
2. Melcer, A.; Klugmann-Radziemska, E.; Lewandowski, W. Phase change materials. Properties, classification, advantages and disadvantages. *Przem. Chem.* **2012**, *91*, 1335–1346.
3. Applications of Phase-Change Materials (PCMs) in Building Engineering. Available online: <https://www.izolacje.com.pl/artykul/sciany-stropy/168194,zastosowania-materialow-zmiennofazowych-pcm-w-budownictwie> (accessed on 2 July 2023).
4. Nabi, H.; Gholinia, M.; Khiadani, M.; Shafieian, A. Performance Enhancement of Photovoltaic-Thermal Modules Using a New Environmentally Friendly Paraffin Wax and Red Wine-rGO/H₂O Nanofluid. *Energies* **2023**, *16*, 4332. [[CrossRef](#)]
5. Poongavanam, P.; Chand, A.A.; Tai, V.B.; Gupta, Y.M.; Kuppusamy, M.; Dhanraj, J.A.; Velmurugan, K.; Rajagopal, R.; Ramachandran, T.; Prasad, K.A.; et al. Annual Thermal Management of the Photovoltaic Module to Enhance Electrical Power and Efficiency Using Heat Batteries. *Energies* **2023**, *16*, 4049. [[CrossRef](#)]
6. Prakash, K.B.; Almeshaal, M.; Pasupathi, M.K.; Chinnasamy, S.; Saravanakumar, S.; Rajesh Ruban, S. Hybrid PV/T Heat Pump System with PCM for Combined Heating, Cooling and Power Provision in Buildings. *Buildings* **2023**, *13*, 1133. [[CrossRef](#)]
7. Li, M.; Yang, Z.; Lu, L.; Yin, K.; Lu, Y. Investigation on Thermal and Electrical Performance of Late-Model Plate-and-Tube in Water-Based PVT-PCM Collectors. *Sustainability* **2023**, *15*, 5988. [[CrossRef](#)]

8. Masood, U.; Haggag, M.; Hassan, A.; Laghari, M. A Review of Phase Change Materials as a Heat Storage Medium for Cooling Applications in the Built Environment. *Buildings* **2023**, *13*, 1595. [[CrossRef](#)]
9. Wieprzkowicz, A.; Heim, D.; Knera, D. Coupled Model of Heat and Power Flow in Unventilated PV/PCM Wall-Validation in a Component Scale. *Appl. Sci.* **2022**, *12*, 7764. [[CrossRef](#)]
10. Rolka, P.; Kwidzinski, R.; Przybylinski, T.; Tomaszewski, A. Thermal Characterization of Medium-Temperature Phase Change Materials (PCMs) for Thermal Energy Storage Using the T-History Method. *Materials* **2021**, *14*, 7371. [[CrossRef](#)]
11. Turski, M.; Jachura, A. Life Cycle Assessment of Dispersed Phase Change Material Heat Accumulators for Cooperation with Buildings in the District Heating System. *Energies* **2022**, *15*, 5771. [[CrossRef](#)]
12. Nowak, K.; Kisilewicz, T.; Berardi, U.; Zastawna-Rumin, A. Thermal Performance Evaluation of a PCM-Integrated Gypsum Plaster Board. *Mater. Proc.* **2023**, *13*, 39. [[CrossRef](#)]
13. Kośny, J.; Thakkar, J.; Kamidollayev, T.; Sobkowicz, M.J.; Trelles, J.P.; Schmid, C.; Phan, S.; Annavajjala, S.; Horwath, P. Dynamic Thermal Performance Analysis of PCM Products Used for Energy Efficiency and Internal Climate Control in Buildings. *Buildings* **2023**, *13*, 1516. [[CrossRef](#)]
14. Amberkar, T.; Mahanwar, P. Review on Thermal Energy Storing Phase Change Material-Polymer Composites in Packaging Applications. *Mater. Proc.* **2021**, *7*, 14. [[CrossRef](#)]
15. Williams, J.D.; Peterson, G.P. A Review of Thermal Property Enhancements of Low-Temperature Nano-Enhanced Phase Change Materials. *Nanomaterials* **2021**, *11*, 2578. [[CrossRef](#)]
16. Mehling, H. Use of Phase Change Materials for Food Applications—State of the Art in 2022. *Appl. Sci.* **2023**, *13*, 3354. [[CrossRef](#)]
17. Yuan, J.; He, P.; Li, H.; Xu, X.; Sun, W. Preparation and Performance Analysis of Ceramsite Asphalt Mixture with Phase-Change Material. *Materials* **2022**, *15*, 6021. [[CrossRef](#)] [[PubMed](#)]
18. Dai, M.; Wang, S.; Deng, J.; Gao, Z.; Liu, Z. Study on the Cooling Effect of Asphalt Pavement Blended with Composite Phase Change Materials. *Materials* **2022**, *15*, 3208. [[CrossRef](#)]
19. Zhou, X.; Kastiukas, G.; Lantieri, C.; Tataranni, P.; Vaiana, R.; Sangiorgi, C. Mechanical and Thermal Performance of Macro-Encapsulated Phase Change Materials for Pavement Application. *Materials* **2018**, *11*, 1398. [[CrossRef](#)]
20. Wilgocka, K.; Krucińska, I.; Skrzetuska, E.; Sujka, W. Investigations of Three-Layer Systems Intended for Protective Clothing for Prematurely Born Babies. *Adv. Mater. Technol.* **2023**, 2300457. [[CrossRef](#)]
21. Wilgocka, K.; Skrzetuska, E.; Krucińska, I.; Sujka, W. Evaluation of Biophysical Properties of Potential Materials for the Manufacture of Protective Garments for Preterm Infants. *Materials* **2022**, *15*, 4878. [[CrossRef](#)]
22. Gadeikytė, A.; Sandonavičius, D.; Rimavičius, V.; Barauskas, R. Finite element analysis of heat and mass exchange between human skin and textile structures. *Balt. J. Mod. Comput.* **2022**, *10*, 159–169. [[CrossRef](#)]
23. Bivainytė, A.; Mikučionienė, D.; Milašienė, D. Influence of the knitting structure of double-layered fabrics on the heat transfer process. *Fibres Text. East. Eur.* **2012**, *20*, 40–43.
24. Miśkiewicz, P.; Tokarska, M.; Frydrych, I.; Makówka, M. Evaluation of thermal properties of certain flame-retardant fabrics modified with a magnetron sputtering method. *Autex Res. J.* **2020**, *21*, 428–434.
25. Miśkiewicz, P.; Tokarska, M.; Frydrych, I.; Makówka, M. Assessment of coating quality obtained on flame-retardant fabrics by a magnetron sputtering method. *Materials* **2021**, *14*, 1348. [[CrossRef](#)] [[PubMed](#)]
26. Miśkiewicz, P.; Tokarska, M.; Frydrych, I. Application of coating mixture based on silica aerogel to improve thermal protective performance of fabrics. *Autex Res. J.* **2022**, *23*, 48–54. [[CrossRef](#)]
27. Puszkarz, A.K.; Machnowski, M.; Błasińska, A. Modeling of thermal performance of multilayer protective clothing exposed to radiant heat. *Heat Mass Transf.* **2020**, *56*, 1767–1775. [[CrossRef](#)]
28. Puszkarz, A.K.; Machnowski, M. Simulations of heat transfer through multilayer protective clothing exposed to flame. *Autex Res. J.* **2020**, *22*, 298–304. [[CrossRef](#)]
29. Krzemińska, S.; Greszta, A.; Bartkowiak, G.; Dąbrowska, A.; Kotas, R.; Pekoślawski, B.; Małachowski, B.; Miśkiewicz, P. Evaluation of Heating Inserts in Active Protective Clothing for Mountain Rescuers—Preliminary Tests. *Appl. Sci.* **2023**, *13*, 4879. [[CrossRef](#)]
30. Machnowski, W.; Waś-Gubała, J. Evaluation of Selected Thermal Changes in Textile Materials Arising in the Wake of the Impact of Heat Radiation. *Appl. Sci.* **2021**, *11*, 6989. [[CrossRef](#)]
31. Renard, M.; Puszkarz, A.K. Modeling of Heat Transfer through Firefighters Multilayer Protective Clothing Using the Computational Fluid Dynamics Assisted by X-ray Microtomography and Thermography. *Materials* **2022**, *15*, 5417. [[CrossRef](#)]
32. Greszta, A.; Bartkowiak, G.; Dąbrowska, A.; Gliścińska, E.; Machnowski, W.; Kozikowski, P. Multilayer Nonwoven Inserts with Aerogel/PCMs for the Improvement of Thermophysiological Comfort in Protective Clothing against the Cold. *Materials* **2022**, *15*, 2307. [[CrossRef](#)]
33. Jansen, K.M.B.; Teunissen, L. Analytical Model for Thermoregulation of the Human Body in Contact with a Phase Change Material (PCM) Cooling Vest. *Thermo* **2022**, *2*, 232–249. [[CrossRef](#)]
34. Santos, G.; Marques, R.; Ribeiro, J.; Moreira, A.; Fernandes, P.; Silva, M.; Fonseca, A.; Miranda, J.M.; Campos, J.B.L.M.; Neves, S.F. Firefighting: Challenges of Smart PPE. *Forests* **2022**, *13*, 1319. [[CrossRef](#)]
35. Młynarczyk, M.; Bartkowiak, G.; Dąbrowska, A. Cooling Effect of Phase Change Materials Applied in Undergarments of Mine Rescuers in Simulated Utility Conditions on Thermal Manikin. *Materials* **2022**, *15*, 1999. [[CrossRef](#)] [[PubMed](#)]

36. Cherunova, I.; Kornev, N.; Lukyanova, E.; Varavka, V. Development and Study of the Structure and Properties of a Composite Textile Material with Encapsulated Heat-Preserving Components for Heat-Protective Clothing. *Appl. Sci.* **2021**, *11*, 5247. [[CrossRef](#)]
37. Bartkowiak, G.; Marszałek, A.; Dąbrowska, A. Thermal Load of Mine Rescuer in the Underwear and Protective Clothing with Phase Change Materials in Simulated Utility Conditions. *Materials* **2020**, *13*, 4320. [[CrossRef](#)] [[PubMed](#)]
38. EN 563; Safety of Machinery—Temperatures of Touchable Surfaces—Ergonomics Data to Establish Temperature Limit Values for Hot Surfaces. ISO: Geneva, Switzerland, 2001.
39. EN ISO 13732-1; Ergonomics of the Thermal Environment—Methods for the Assessment of Human Responses to Contact with surfaces—Part 1: Hot Surfaces. ISO: Geneva, Switzerland, 2009.
40. EN ISO 6942; Protective Clothing—Protection against Heat and Fire—Method of Test: Evaluation of Materials and Material Assemblies When Exposed to a Source of Radiant Heat. ISO: Geneva, Switzerland, 2002.

Disclaimer/Publisher’s Note: The statements, opinions and data contained in all publications are solely those of the individual author(s) and contributor(s) and not of MDPI and/or the editor(s). MDPI and/or the editor(s) disclaim responsibility for any injury to people or property resulting from any ideas, methods, instructions or products referred to in the content.